Original Article

Institution of MECHANICAL ENGINEERS
Journal of ENGINEERING IN MEDICINE

Proc IMechE Part H:
J Engineering in Medicine
2019, Vol. 233(11) 1141–1150

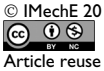

DOI: 10.1177/0954411919876466
journals.sagepub.com/home/pih
SAGE

Mechanical Follow-the-Leader motion of a hyper-redundant surgical instrument: Proof-of-concept prototype and first tests

Paul WJ Henselmans, Gerwin Smit and Paul Breedveld

Abstract

One of the most prominent drivers in the development of surgical procedures is the will to reduce their invasiveness, attested by minimally invasive surgery being the gold standards in many surgical procedures and natural orifices transluminal endoscopic surgery gaining acceptance. A logical next step in this pursuit is the introduction of hyper-redundant instruments that can insert themselves along multi-curved paths referred to as Follow-the-Leader motion. In the current state of the art, two different types of Follow-the-Leader instruments can be distinguished. One type of instrument is robotized; the movements of the shaft are controlled from outside the patient by actuators, for example, electric motors, and a controller storing a virtual track of the desired path. The other type of instrument is more mechanical; the movements of the shaft are controlled from inside the patient by a physical track that guides the shaft along the desired path. While in the robotized approach all degrees of freedom of the shaft require an individual actuator, the mechanical approach makes the number of degrees of freedom independent from the number of actuators. A desirable feature as an increasing number of actuators will inevitably drive up costs and increase the footprint of an instrument. Building the physical track inside the body does, however, impede miniaturization of the shaft's diameter. This article introduces a new fully mechanical approach for Follow-the-Leader motion using a pre-determined physical track that is placed outside the body. This new approach was validated with a prototype called MemoFlex, which supports a Ø5 mm shaft (standard size in minimally invasive surgery) that contains 28-degrees-of-freedom and utilizes a simple steel rod as its physical track. Even though the performance of the MemoFlex leaves room for improvement, especially when following multiple curves, it does validate the proposed concept for Follow-the-Leader motion in three-dimensional space.

Keywords

minimally invasive surgery, natural orifices transluminal endoscopic surgery, surgical instruments, Follow-the-Leader, pathway surgery, hyper-redundant, snake-like, tendon-driven

Date received: 01 May 2019; accepted: 26 August 2019

Introduction

Minimally invasive surgery (MIS) strives to reduce the invasiveness of surgical procedures by limiting the size of the required incisions. With its obvious benefits of less scar tissue, faster recovery time and less complications, MIS has gained broad acceptance. The currently used instruments for MIS are slender (max Ø5 mm) and predominantly straight and rigid. Due to their rigidity, the path from incision to operative area must be a straight line. This can pose a problem as the human anatomy consists of organic shapes and a tortuous network of nerves and vessels, through which a straight path is not always an option. Work-arounds exist, for example, the abdomen can be inflated to increase the amount of workspace. However, such methods are not applicable in more dense areas in the human body, for example, the skull base, reducing the possibilities for

Department of Biomechanical Engineering, Faculty of Mechanical, Maritime and Materials Engineering, Delft University of Technology, Delft, The Netherlands

Corresponding author:
Paul WJ Henselmans, Department of Biomechanical Engineering, Faculty of Mechanical, Maritime and Materials Engineering, Delft University of Technology, Mekelweg 2, 2628 CD Delft, The Netherlands.
Email: p.w.j.henselmans@tudelft.nl

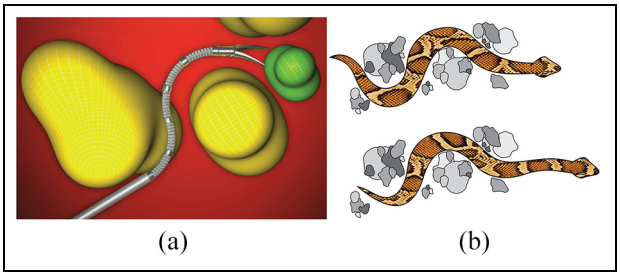

Figure 1. Follow-the-Leader motion. (a) Artistic representation of a Follow-the-Leader instrument used to avoid obstacles. (b) Snake navigating through cluttered environment by steering its head and maneuvering its body along the created path using Follow-the-Leader motion.

easy reach of the operative area. Therefore, MIS-instruments are ideally not rigid but flexible, allowing them to curve along with the anatomy of the human body. Passive flexible instruments, such as, for example, catheters or colonoscopes, can only be used to move along existing anatomic pathways such as blood vessels or intestines. Reaching less accessible locations within the human body implies a need for active flexible instruments with an actively controllable shape, allowing steering along multi-curved paths along vulnerable anatomy (Figure 1(a)).[1,2]

Instruments that contain such active flexibility are referred to as hyper-redundant, a term first coined by the field of robotics.[3] The term hyper-redundant reflects the fact that these type of devices contain more degrees of freedom (DOFs) than is strictly necessary for maneuvering their end-effector. These additional DOFs allow a hyper-redundant instrument to actively re-shape its shaft, a useful feature for maneuvering within a spatially restricted environment.

A hyper-redundant instrument enables so-called Follow-the-Leader (FTL) motion, which is comparable to a type of forward locomotion of a snake (Figure 1(b)).[4] In this comparison, the head of the snake is regarded as the leader, which is steered, for example, to maneuver along the stones of Figure 1(b). As the snake moves forward, the body follows the curved path initiated by the head. In this way, FTL motion allows motion along multi-curved pathways, while reducing the required access (i.e. the width of the path) to a minimum. These characteristics make FTL motion especially suitable for natural orifice transluminal endoscopic surgery (NOTES) wherein natural orifices such as the nose, mouth or anus are used as the surgical entry point.[5,6] A good example being endoscopic endonasal surgery (EES) wherein the instrument enters through the nose in order to reach the skull base.[7,8] The skull base contains a network of blood vessels, nerves and other delicate structures and the surgical workspace is limited ($105.1 \times 76.2 \times 51.9$ mm)[9]. As a result, some areas remain inaccessible by straight instruments and FTL instrumentation could extend the reach of the procedure.

State of the art

Several approaches to FTL motion of medical instruments have been proposed in the literature. They will be discussed based on how these approaches affect the diameter of the shaft and its level of redundancy. A division is made between robotized instruments that use a virtual track and more mechanical instruments that build a physical track.

Instruments using a virtual track

Literature contains a number of robotized systems that store a virtual track of the desired path on a computer.[2] The computer controls every DOF of the hyper-redundant shaft via individual actuators, which are either embedded in the shaft or placed at the instrument's base outside the patient.[10–15] Instruments with actuators at their base are easiest to miniaturize, the thinnest one currently existing having a diameter of Ø8 mm.[14] A drawback of using a computerized virtual track is that every DOF of the hyper-redundant shaft must be controlled by an individual actuator, with ten being the maximum found number of DOFs in literature of medical instruments.[13] As the level of redundancy within the shaft directly relates to the complexity of the path, that is, more DOFs allows a more tortuous path, the allowed complexity of the path becomes directly dependent on the number of actuators in the system. This is an undesirable feature as increasing the number of actuators will inevitably drive up costs and require more space near the patient in the workspace of the surgeon.

Instruments using a physical track

There are FTL instruments that contain less actuators than the number of DOF in their hyper-redundant shafts, reducing the overall complexity of the system.[16–20] The thinnest ones being the concentric tube robots or active cannulas, first developed by Webster et al. at Vanderbilt University and since then extensively researched by others.[21–24] Their shafts consists of a telescoping mechanism of pre-curved, compliant, thin-walled tubes, with diameters ranging from 0.8 to 2.4 mm depending on the application.[25] Translating and rotating these compliant tubes relative to one another causes them to interact and deform, changing the overall shape of the shaft. FTL motion can be achieved by modelling the interaction between the pre-curved tubes, and planning the required control sequence for shaft motion.[26,27] The pre-defined curves of these tubes, however, limit the FTL motion to a restricted set of highly specific pre-planned paths. There are instrument that are capable of FTL motion along a wider array of non-specific paths, the most promising being the highly articulated robotic probe (HARP, and also known as CardioArm), developed by Ota et al.[17–19] and commercialized as the Flex Robotic

System by Medrobotics.[28] Its shaft consists of two arms that are placed concentrically within each other. Both arms can independently advance forward and switch between a flexible and locked state. FTL motion is achieved by letting the arms alternate between flexible and locked, while the locked arm memorizes the current shape of the system and serves as a guide for the flexible arm that advances forward and is steered in a new direction. The shaft has an impressive 105-DOFs, while the HARP only needs six actuators for steering, locking, and advancing its arms.[17,29] In this way, level of redundancy of its shaft becomes independent of the number of actuators.

The HARP showcases an interesting approach to FTL motion: where normally a computer stores a virtual track of the path and drives a set of actuators, one for each DOF, the HARP builds a physical track inside its body that guides the motion. Consequently, the level of redundancy within the shaft, and thus, the complexity of the paths that can be followed, becomes independent from the number of actuators. Nevertheless, building the physical mechanical track inside the shaft impedes miniaturization of the diameter of the HARP, which is currently Ø10 mm.[17,18]

This article introduces a new approach for an FTL instrument that uses a physical mechanical track placed outside of the shaft, that is, at the user-side of the instrument that does not enter the patient and for this reason is less bound to the severe diameter restrictions for minimally invasive shafts. In this way, the DOFs of its hyper-redundant shaft become independent from the number of actuators, while the shaft's diameter can be miniaturized to a MIS standard of Ø5 mm.

A new approach

The basic principle of the proposed approach is illustrated in Figure 2(a). The general setup contains two similar structures, the master and the slave, each consisting of jointed segments stacked in series to form a flexible structure. All segments are connected to a pair of cables. The function of the master is to follow a physical track located outside the patient's body. The function of the slave is to copy the movements of the master, and in this way propagate along the desired path inside the patient's body.

For the slave to copy the movements of the master, its cables need to be coupled to those of the master. The function of the cables is to transfer the forces that are generated in the master to the slave. Directly coupling a cable in the master to its equivalent cable in the slave is, however, not possible. This has to do with the fact that the master is forced into the desired shape by the track, while the slave is forced into that same shape by the cables. Consequently, equivalent cables in the master and slave will travel the same distance, yet the tensions in the cables should be reversed, that is, a cable that is pulled in the master should be released in the slave and vice versa, as indicated in Figure 2(a). There is however a simple work-around. As proven in Figure 2(b), if a cable is assumed to bend with a constant radius within a segment, the absolute length changes of its antagonist cable is equal to each other. This means that a cable in the master and its antagonist in the slave travel the same distance with tension in the same direction. It is therefore possible to connect a cable of the master to its antagonist in the slave. The result is something like the hypothetical configuration illustrated in Figure 2(c), were a rigid U-shaped shaft was added to connect the master to the slave and to guide the cables.

Even though the U-shaped configuration of Figure 2(c) could function in theory, there are two downsides of using a U-shaped shaft as compared to a more conventional straight shaft. First of all, the cables will experience additional friction as they change direction through the bend. Second, a U-shaped instrument is rather inconvenient during a surgical procedure as it blocks the workspace in front of the patient. For these reasons, a straight shaft is preferred.

In Figure 3(a), the direction of the master is rotated over 180° to enable the inclusion of a straight shaft. The track is in this configuration also rotated over 180° in a mirrored direction opposite to the path. As a result, the shaft must telescopically extend so that the master can move backward along the mirrored track while the slave moves forward along the path. An extending shaft is, however, an impractical solution as the cables running through the shaft then need to extend as well.

The extending shaft in Figure 3(a) was necessary because both the track and path were considered stationary. However, while the path, for obvious reasons, has to remain stationary, the track does not. Therefore, the track can be moved relative to the instrument, avoiding the need for an extending shaft. This principle is visualized in Figure 3(b), where the shaft is straight and has a fixed length. The movement is now considered from the point of view of the slave. For the slave to travel a distance Δs over the path, the master must travel the same distance over the track. Because the master is now rigidly connected to the slave, it moves along with the slave away from the track with distance Δs. As a consequence, the track must travel twice the distance Δs relative to the stationary path, that is, the speed of the track must be double the speed of the instrument. Thus, the opposite direction between track and path can be compensated by pulling the track through the master at double the speed of the instrument.

Figure 3(c) shows a schematic mechanism of gears and gear racks that double the speed of the track compared to the instrument. The instrument is connected to the centre of the gears, which run forward over a stationary gear rack. The track is connected to a gear rack (red) that connects to the top of the gears. In this way, the speed of the track will always be double the speed of the instrument.

Proof of concept

In order to validate the concept of Figure 3(c), a proof-of-concept (PoC) prototype was developed based on the following requirements. The prototype should be steerable in two planes to allow movement in 3D space. Both the master and slave should be axially and torsionally stiff, while having a low bending stiffness. The slave should support an inner-channel to provide functionality, for example, a tube for suction, a fibre for vision, or cable for actuation of an end-effector. The diameter of the slave should stay within Ø5 mm, a typical dimension for MIS instruments. Our PoC prototype was developed for validating the functionality of the proposed concept, and not for direct use in a medical setting. Requirements as biocompatibility, sterilizability, and integration into current medical protocols and procedures were therefore not yet addressed.

Master design

For the track, a bendable stainless steel rod with a diameter of Ø3 mm was chosen. For the master to capture the shape of the sliding track, a flexible 'track-follower' structure in the master is required. A possible track-follower structure is illustrated in Figure 4(a), wherein a set of rings are slid over the track. Each ring sits perpendicular to the centreline of the track, and thus, copies the angle of the track at that specific position. By placing multiple rings at fixed intervals along the length of the track, the shape of the track is captured.

The track-follower structure in Figure 4(a) has a few downsides. First, it is difficult to guarantee that the rings remain perpendicular to the centreline of the track, especially if the rings are thin. A ring that sits oblique to the track's centreline, that is, not perfectly perpendicular, will lead to an inaccurate copy of the shape of the track and can result in jamming, resulting in blockage of the track when it is pulled through the rings. Making the rings thick as to avoid jamming is not an option, as steep curves in the track would then no longer fit through the holes in the rings. In a search for a better alternative we started considering using a helical structure (Figure 4(b)). A helical structure has a single point of contact at any cross section along the track, making it impossible to grip onto the track, thus avoiding any possibility of jamming. Moreover, similar to a compression spring, a helical will be able to bend along with the curvature of the track, and in this way capture the shape of the track in a continuous manner. However, one helical alone does not encircle the track at every cross section, reducing the resolution of the captured shape. We therefore decided to use three helices placed at 120° intervals along the circumference of the track, Figure 4(c). This structure was 3D printed and shown in Figure 4(d) together with the Ø3 mm bent steel rod that forms the track.

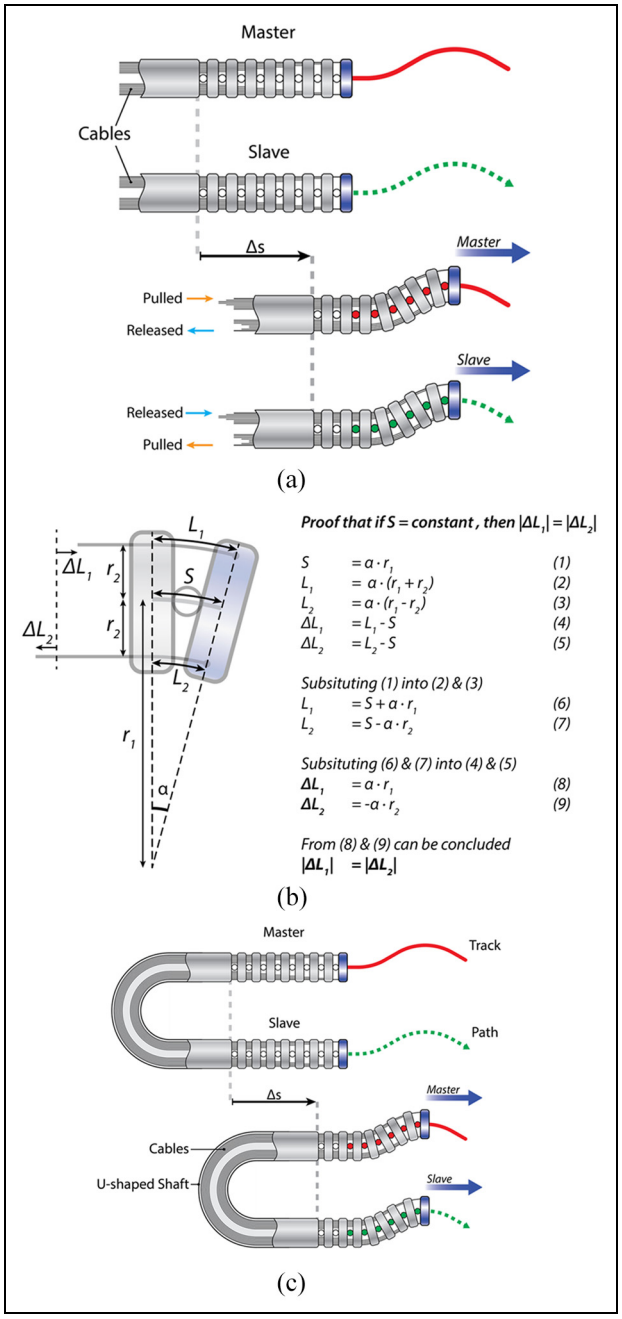

Figure 2. Schematic representation of a new approach for a Follow-the-Leader instrument. (a) The instrument containing a master that follows a physical track located outside the patient's body, and a slave that copies the movement of the master and propagates along the path inside the patient's body. The 'Released' and 'Pulled' arrows indicate the tension in the cables of the first segment. (b) Length behaviour of antagonist cables L1 and L2. If the length of the segment S is fixed and the cables are presumed to bend with a constant radius, the absolute length changes|ΔL1| and|ΔL2| of antagonistic cables are equal. (c) Hypothetical instrument. The cables in the master are coupled to their antagonists in the slave. A U-shaped shaft connects the master to the slave, and guides the cables.

Next to the ability to capture the shape of the track, the master needs to be axially stiff, torsionally

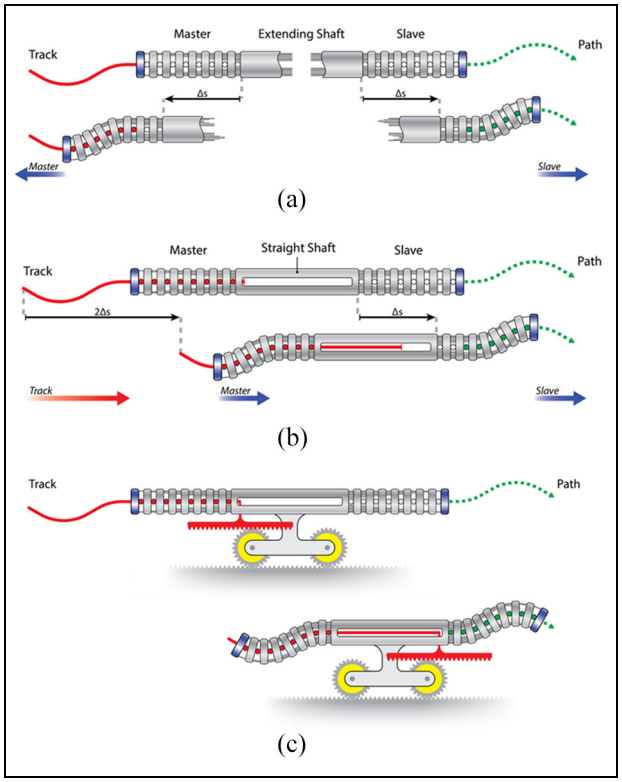

Figure 3. Straight configuration. (a) Improved configuration of Figure 2(c). With a straight shaft, the track and path face in the opposite direction. To allow the master to move forward over the track while the slave moves forward over the path, the shaft and cables need to extend. (b) Improved configuration of Figure 3(a) avoiding the extension of the shaft. Master and slave rigidly connected by the shaft. The track is given double the speed of the instrument to compensate for the opposite direction between track and path. (c) A mechanism of gears and gear racks pulls the track through the master at double the speed of the instrument.

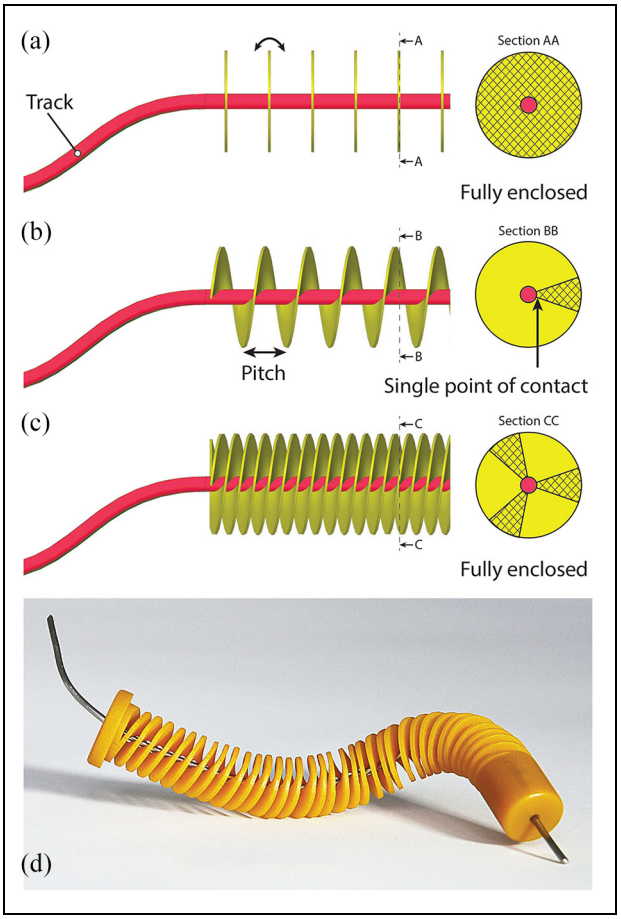

Figure 4. Three track-followers. (a)–(c) Structures to capture the shape of a track. For further explanation, see text. (d) Track-follower based on three helices conforming to the shape of a Ø3 mm track represented by a bent steel rod. 3D printed from the flexible material ABFlex on an Envisiontec Perfactory 4.

stiff, have a low bending stiffness, and guide the cables. As the helical track-follower of Figure 4(d) is not axially stiff, it was enclosed by an exoskeleton as illustrated in Figure 5(a). The exoskeleton is composed out of a series of rings that enclose the track-follower and are connected to each other in a way that they form a sequence of universal joints. The cables are guided through holes in the rings and fixed by screws at the desired spot. By using an exoskeleton with a universal-joint construction, axial and torsion stiffness is provided without adding additional bending stiffness to the master.

Slave design

The slave was constructed following the principle of the squid-inspired cable-ring mechanism applied in a range of surgical instrument prototypes developed at the Bio-Inspired Technology (BITE)-group at TU Delft.[30,31] Stranded stainless steel cables with a diameter of Ø0.2 mm were arranged in a Ø4.5 mm cable-ring, allowing space for a total of 56 cables. Each segment is controlled in 2-DOFs by four cables, enabling a total of 56/4 = 14 segments and motion in 28-DOFs. The outside diameter of the slave (d_s) is Ø5 mm, and the length of each segment was chosen to be 8 mm, resulting in a total slave length of 112 mm. Figure 5(b) shows the construction of the slave. The segments are connected to each other via a series of hex-ball joints. These joints allow for bending with zero stiffness, while providing the necessary axial and torsion stiffness. Every segment contains two hex-ball joints allowing all together a maximum bend of 60°. The cables were glued into the grooves at the circumference of the segments, and springs enclose the cable-ring and provide guidance to the cables.

PoC prototype: MemoFlex

Figure 5(c) shows the entire PoC prototype named MemoFlex. The master and slave are connected to each other via a rigid shaft. The shaft accommodates the increase in diameter of the cable-ring from slave (Ø4.5 mm) to master (Ø18 mm) by guiding the cables

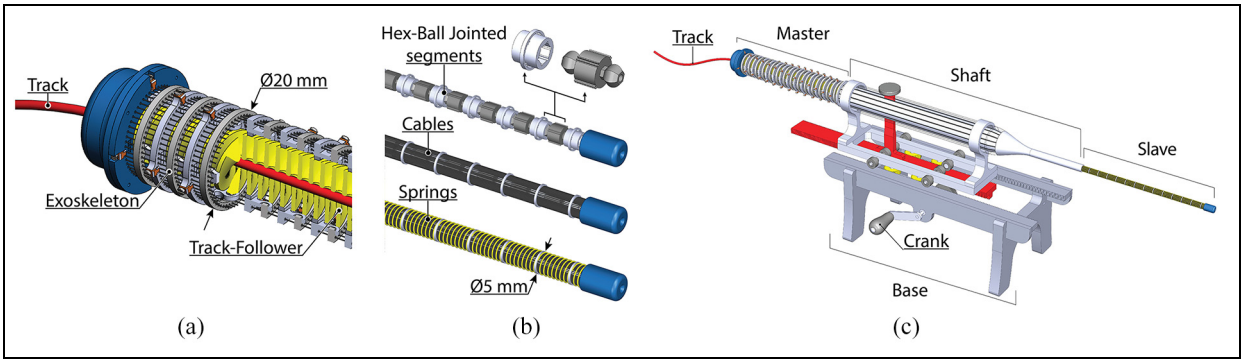

Figure 5. Computer-aided design (CAD) drawings of PoC instrument. (a) The master consisting of the helical track-follower and an axial and torsion stiff exoskeleton that fixates and guides the cables. (b) The construction of the Ø5 mm, 112 mm long slave containing 14 segments providing a total of 28-DOFs. (c) CAD drawing of the completed MemoFlex prototype. The cable ring diameter in the master (Ø18 mm) is four times larger than the cable ring diameter in the slave (Ø4.5 mm). This results in an amplification factor four between the motion of master and slave, for example, a 5° bend in the master will result into a 20° bend in the slave.

through grooves at its surface. The increase in diameter spreads the cables outward, creating space to reach the track within the shaft, as proposed in Figure 3(c). The master and slave both have a length of 112 mm, and the entire length of the instrument is 500 mm. The supporting base contains a gearing mechanism to ensure that, upon manually turning a crank, the instrument moves forward while the track is pulled through the master at double the speed.

Performance test

The MemoFlex was successfully fabricated as illustrated in Figure (6). Its performance was evaluated using two different tracks: a single curve (C-curve) and a double curve (S-curve). The results of these test are illustrated in Figure 7(a), which shows the slave at three positions (insertion, halfway and final position), and an overlay of intervals of approximately 10 mm during forward motion. The blue cap on the tip of the slave not an actively driven segment, but is solely used for storing the cable-endings and is expected to sway long with the motion. Accurate FTL performance would result in the total width of the slave's footprint to be as close as possible to the diameter of the slave.

From Figure 7(a) it is clear that MemoFlex can follow a C-curve reasonably well, with the maximum width of the slave's footprint being approximately three times the diameter of the slave ($3d_s$), including the blue cap. Figure 7(a) also shows the performance in following an S-curve, which is considerably worse. In its end-position, the slave does mimic the desired S-shape, yet during the motion the slave strays away from the path. The maximum footprint of the slave is approximately $8d_s$.

The line of insertion in Figure 7(a) represents the point after which the segments become actively driven towards the desired shape. The segments after this line are referred to as driven segments, while the segments before this line are referred to as non-driven segments. The non-driven segments should remain in a straight position. Especially at the halfway position of the S-curve, it is clear that this is not the case, as the non-driven segments bend along in the direction of the driven segments. This is avoidable by supporting the slave at the line of insertion. In Figure 7(b), the slave is again following the S-curve, but now a part referred to as the insert guided is added to the setup. The insert guide is basically a ring fixed to the ground that encloses and supports the slave. By comparing the halfway position of the S-curve in Figure 7(b) to the halfway position of the S-curve of Figure 7(a), it is clear that adding the insert guide improved performance. The non-driven segments are no longer able to move along with the driven segments, and the maximum footprint of the slave has decreased from $8d_s$ to approximately $5d_s$.

Stiffness

Stiffness is an important measure for the functionality of a surgical instrument, as it determines the forces an instrument to be applied. The stiffness of the slave was measured at its tip by pulling the slave upwards using an analogue force gauge. This measurement was done with the slave in two different positions; the initial straight position and the end-position of the S-curve. The stiffness at the initial position was measured to be 0.01 N/mm (0.2 N over a distance of 18 mm), and the stiffness at the end-position was measured to be 0.06 N/mm (0.6 N over a distance of 10 mm). Due to hysteresis as a result of friction and play within the system, the slave did not return to its initial position after completing the measurement. In the straight position, this resulted in a deviation of 7 mm from the initial position. In the end-position of the S-curve, this resulted in a deviation of 1 mm from the initial position. The differences between the measurements on the straight position and the end-position can be explained

Figure 6. Proof-of-concept prototype; the MemoFlex. All parts were fabricated out of aluminium, except for the wheels (nylon), gear rack (stainless steel) and gears (brass). The outside of the shaft is transparent to allow visual feedback of the cables during their assembly.

by the fact that in the straight position the cables are not yet used for actuation. As a result, the tension in the cables will be lower and the cables can even be slack, which directly affects the stiffness of the slave and the amount of hysteresis in the system.

Discussion

The MemoFlex shows that the proposed concept of using a physical track placed outside the shaft is viable, and allows the diameter of the shaft to be miniaturized to Ø5 mm. However, improvements are necessary to generate satisfying results. The main cause of error was identified to be the non-driven segments diverting from their straight path. A solution was found in supporting the slave at the line of insertion. Although this enhanced its performance significantly, there is still room for improvement.

The performance of the MemoFlex is considerably affected by mechanical losses in the system. These loses were especially noticeable in the form of hysteresis during the stiffness measurement on the straight position of the slave. The losses can mainly be described to friction in the joints of the slave and master, and friction and play between the cables and their guiding components. Although the fully mechanical nature of the MemoFlex makes it impossible to completely prevent or compensate for such losses, they can be minimized. An interesting approach would be to use a continuous instead of a rigid-linked construction in the master and slave. In this way, the joints are replaced by a compliant backbone, eliminating the friction in the joints. Moreover, a continuous approach will allow the cables to be guided more fluently, which can have a positive effect on the play and friction between the cables and their guiding components.

NOTES

The technique of the MemoFlex could have various applications in NOTES, though its current dimensions especially suite the surgical workspace of EES. The presented C-curve could, for example, reach the anterior cranial fossa via the endonasal approach, an area that can be problematic with straight instruments.[32] The S-curve could, for example, be used to approach the pituitary at a different angle or possibly even reach behind it. The MemoFlex will, however, not be able to perform all tasks due to its limited stiffness. The applied forces during tasks as soft tissue interaction or bony interaction at the skull base were measured to be 0.13 and 0.82 N, respectively.[33] In its current form, the MemoFlex is not stiff enough to exert such forces without considerable deflection. Moreover, a brake should be installed on the gearing mechanism, as the entire instrument can now be pushed backward due to external loading. The MemoFlex will be able to perform tasks that do not require high forces at the tip such a visualization and suction.

Future developments

The MemoFlex prototype is the first step in the development of fully mechanical instruments capable of FTL motion. Even though the results were not fully satisfactory, the prototype's behaviour does show the viability of the proposed concept and it can be concluded that the flaws arise from the implementation rather than from the concept itself. In general, a fully mechanical approach has some advantages for medical applications compared to robotized systems. For one, eliminating the need for a computer reduces the instrument's footprint in the already crowded operation room. Moreover, eliminating the need for actuators decreases the size of the master, taking up less space in the surgeons working area close to the patient. Furthermore, the absence of electric components could considerably drive down the costs of production. That said, the higher level of control offered by robotized systems can produce more accurate results. Future

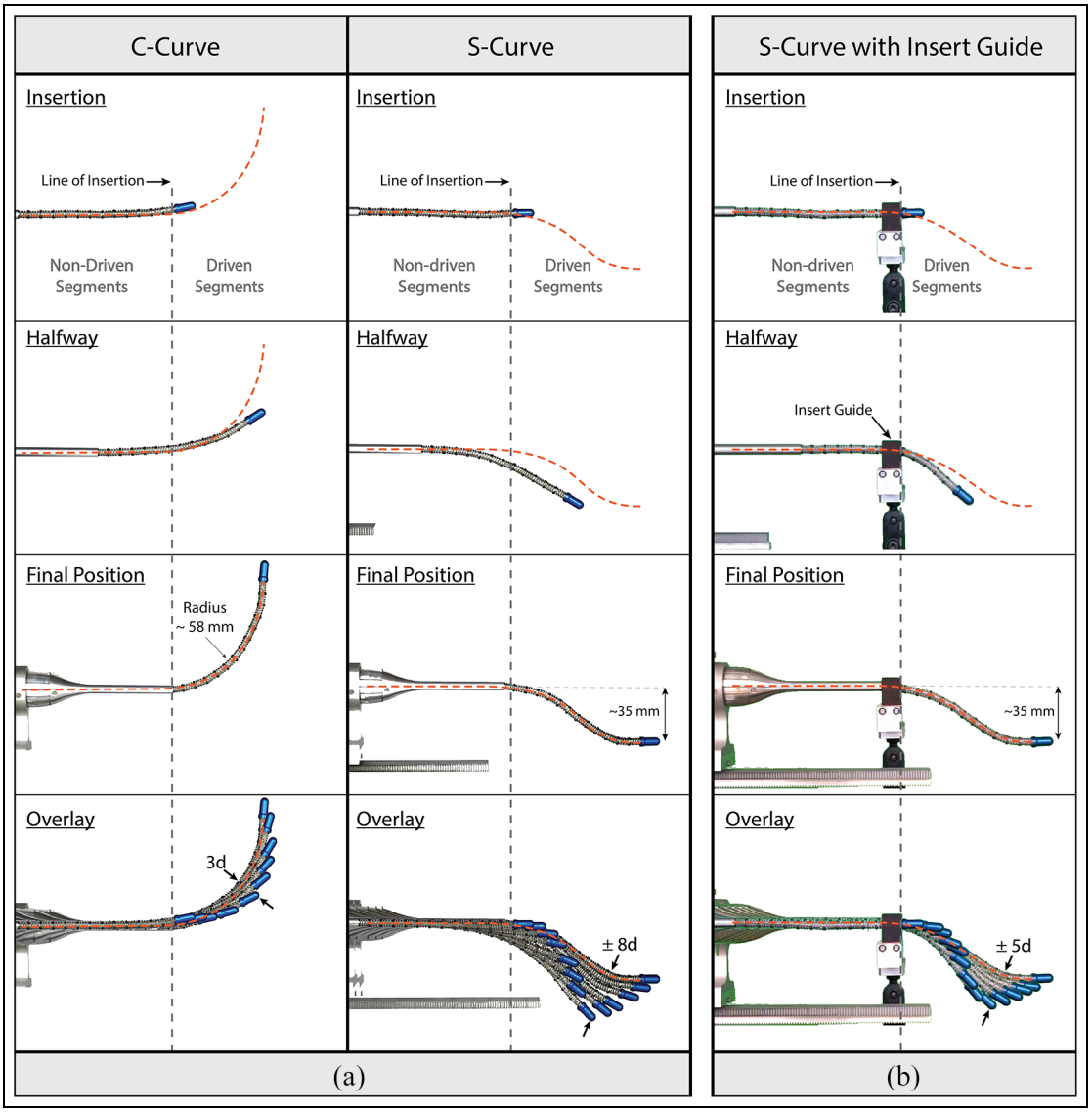

Figure 7. Evaluation of the MemoFlex showing the movement of the slave. (a) From left to right, the slave following a C-curve with a radius of ±58 mm and a footprint of $\pm 3d_s$, and S-curve with a step of ±35 mm and a footprint of $\pm 8d_s$. The orange striped line indicates the path. (b) The slave following a S-curve while supported by the insert guide with a step of ±35 mm and a footprint of $\pm 5d_s$.

research will have to show if a sufficient level of accuracy is attainable by a fully mechanical approach.

A next step in the development of the MemoFlex will be focused on adapting a continuous approach to the design of the master and slave. The compliant track-follower could, for example, be expanded to also serve as a guidance for the cables in the master. Moreover, this structure could then be extended towards the slave, paving the way to an all-in-one piece 3D printed instrument. 3D printing can also prove to be useful for the fabrication of patient-specific tracks. The shape of the track would be based on a path planned prior to surgery by a physician based on computerized tomography (CT) or magnetic resonance imaging (MRI) images. This 3D track could then be printed from a stiff material, for example, stainless steel. Future developments will thus be focused on the use of 3D printing, and we envision that, combined with the absence of electrical components, this could considerably drive down the costs of production and potentially lead to a fully disposable FTL solution.

Conclusion

This article introduces a novel fully mechanical approach for FTL motion of a hyper-redundant surgical instrument. To eliminate the need for a single actuator per DOF of a hyper-redundant instrument, the approach includes the use of a physical track. This track was placed outside the patient to allow for the miniaturization of the instruments' diameter. The proposed technique was implemented in a prototype called MemoFlex supporting a hyper-redundant shaft with a diameter of 5 mm and 28-DOFs. MemoFlex showed

the validity of the proposed technique, and its evaluation showed higher accuracy for following C-curves (footprint of the path ~3 times the instrument's diameter ($3d_s$)) than for S-curves (~$8d_s$). The performance for S-curves was improved by supporting the shaft at the point of insertion (~$5d_s$).

Acknowledgements

The authors thank technician David Jager from the DEMO Central Workshop of Delft University of Technology for the fabrication of the prototype.

Author contributions

PWJH and PB conceived and designed the analysis. PWJH collected the data. All authors contributed in performing the analysis and writing the paper.

Declaration of conflicting interests

The author(s) declared no potential conflicts of interest with respect to the research, authorship, and/or publication of this article.

Funding

The author(s) disclosed receipt of the following financial support for the research, authorship, and/or publication of this article: This work is part of the research programme 'Bio-Inspired Maneuverable Dendritic Devices for Minimally Invasive Surgery' with Project Number 12137, which is financed by the Netherlands Organisation for Scientific Research (NWO).

ORCID iDs

Paul WJ Henselmans https://orcid.org/0000-0003-2031-8561
Gerwin Smit https://orcid.org/0000-0002-8160-3238

References

1. Burgner-Kahrs J, Rucker DC and Choset H. Continuum robots for medical applications: a survey. *IEEE T Robot* 2015; 31(6): 1261–1280.
2. Loeve A, Breedveld P and Dankelman J. Scopes too flexible and too stiff. *IEEE Pulse* 2010; 1(3): 26–41.
3. Chirikjian GS. *Theory and applications of hyper-redundant robotic manipulators*. PhD Dissertation, California Institute of Technology, Pasadena, CA, 1992.
4. Choset H and Henning W. A follow-the-leader approach to serpentine robot motion planning. *J Aerospace Eng* 1999; 12(2): 65–73.
5. Atallah S, Martin-Perez B, Keller D, et al. Natural-orifice transluminal endoscopic surgery. *Brit J Surg* 2015; 102(2): e73–e92.
6. Arkenbout E, Henselmans PJ, Jelínek F, et al. A state of the art review and categorization of multi-branched instruments for NOTES and SILS. *Surg Endosc* 2015; 29(6): 1281–1296.
7. Cappabianca P, Cavallo LM and De Divitiis E. Endoscopic endonasal transsphenoidal surgery. *Neurosurgery* 2004; 55(4): 933–940.
8. Cappabianca P, Cavallo LM, Esposito F, et al. Extended endoscopic endonasal approach to the midline skull base: the evolving role of transsphenoidal surgery. *Adv Tech Stand Neurosurg* 2008; 33: 151–199.
9. Burgner J, Swaney PJ, Rucker DC, et al. A bimanual teleoperated system for endonasal skull base surgery. In: *2011 IEEE/RSJ international conference on intelligent robots and systems*, San Francisco, CA, 25–30 September 2011, pp.2517–2523. New York: IEEE.
10. Waye JD. Quo vadis: another new colonoscope. *Am J Gastroenterol* 2007; 102(2): 267–268.
11. Shang J, Noonan DP, Payne C, et al. An articulated universal joint based flexible access robot for minimally invasive surgery. In: *2011 IEEE international conference on robotics and automation*, Shanghai, 9–13 May 2011, pp.1147–1152. New York: IEEE.
12. Tappe S, Pohlmann J, Kotlarski J, et al. Towards a follow-the-leader control for a binary actuated hyper-redundant manipulator. In: *2015 IEEE/RSJ international conference on intelligent robots and systems*, Hamburg, 28 September–2 October 2015, pp.3195–3201. New York: IEEE.
13. Son J, Cho CN, Kim KG, et al. A novel semi-automatic snake robot for natural orifice transluminal endoscopic surgery: preclinical tests in animal and human cadaver models (with video). *Surg Endosc* 2015; 29(6): 1643–1647.
14. Neumann M and Burgner-Kahrs J. Considerations for follow-the-leader motion of extensible tendon-driven continuum robots. In: *2016 IEEE international conference on robotics and automation (ICRA)*, Stockholm, 16–21 May 2016, pp.917–923. New York: IEEE.
15. Palmer D, Cobos-Guzman S and Axinte D. Real-time method for tip following navigation of continuum snake arm robots. *Robot Auton Syst* 2014; 62(10): 1478–1485.
16. Kang B, Kojcev R and Sinibaldi E. The first interlaced continuum robot, devised to intrinsically follow the leader. *PLoS ONE* 2016; 11(2): e0150278.
17. Ota T, Degani A, Schwartzman D, et al. A highly articulated robotic surgical system for minimally invasive surgery. *Ann Thorac Surg* 2009; 87(4): 1253–1256.
18. Rivera Serrano CM, Johnson P, Zubiate B, et al. A transoral highly flexible robot. *Laryngoscope* 2012; 122(5): 1067–1071.
19. Johnson PJ, Rivera Serrano CM, Castro M, et al. Demonstration of transoral surgery in cadaveric specimens with the medrobotics flex system. *Laryngoscope* 2013; 123(5): 1168–1172.
20. Amanov E, Granna J, Burgner-Kahrs J, et al. Toward improving path following motion: hybrid continuum robot design. In: *2017 IEEE international conference on robotics and automation (ICRA)*, Singapore, 29 May–3 June 2017, pp.4666–4672. New York: IEEE.
21. Dupont PE, Lock J, Itkowitz B, et al. Design and control of concentric-tube robots. *IEEE T Robot* 2010; 26(2): 209–225.
22. Gilbert HB, Rucker DC and Webster RJIII. Concentric tube robots: the state of the art and future directions. In: Inaba M and Corke P. (eds) *Springer tracts in advanced robotics*. Cham: Springer, 2016, pp.253–269.

23. Burgner J, Rucker DC, Gilbert HB, et al. A telerobotic system for transnasal surgery. *IEEE T Mech* 2014; 19(3): 996–1006.
24. Mahoney AW, Gilbert HB and Webster RJIII. A review of concentric tube robots: modeling, control, design, planning, and sensing. In: Patel R (ed.) *The encyclopedia of medical robotics*. Singapore: World Scientific, 2018, pp.181–202.
25. Webster RJ, Okamura AM, Cowan NJ, et al. Toward active cannulas: miniature snake-like surgical robots. In: *2006 IEEE/RSJ international conference on intelligent robots and systems*, Beijing, 9–15 October 2006, pp.2857–2863. New York: IEEE.
26. Gilbert HB and Webster RJ and editors. Can concentric tube robots follow the leader ? In: *Proceedings – IEEE international conference on robotics and automation*, Karlsruhe, 6–10 May 2013, pp.4881–4887. New York: IEEE.
27. Gilbert HB, Neimat J and Webster RJ. Concentric tube robots as steerable needles: achieving follow-the-leader deployment. *IEEE T Robot* 2015; 31(2): 246–258.
28. Medrobotics Corporation. Flex robotic system, Raynham, Massachusetts: Medrobotics, 2019, https://medrobotics.com
29. Henselmans PW, Gottenbos S, Smit G, et al. The memo-slide: an explorative study into a novel mechanical follow-the-leader mechanism. *P I Mech Eng, Part H: J Eng Med* 2017; 231(12): 1213–1223.
30. Breedveld P, Sheltes JS, Blom EM, et al. A new, easily miniaturized steerable endoscope. *IEEE Eng Med Biol* 2005; 24(6): 40–47.
31. Breedveld P and Scheltes JS. Instrument for fine-mechanical or surgical applications (*Google Patents*), 2005, https://repository.tudelft.nl/islandora/object/uuid:2bc4b08c-246f-4504-8bc1-8d866a943b33?collection=research
32. Liu JK, Christiano LD, Patel SK, et al. Surgical nuances for removal of olfactory groove meningiomas using the endoscopic endonasal transcribriform approach. *Neurosurgl Focus* 2011; 30(5): E3.
33. Bekeny JR, Swaney PJ, Webster RJ, et al. Forces applied at the skull base during transnasal endoscopic transsphenoidal pituitary tumor excision. *J Neurol Surg Part B Skull Base* 2013; 74(6): 337–341.